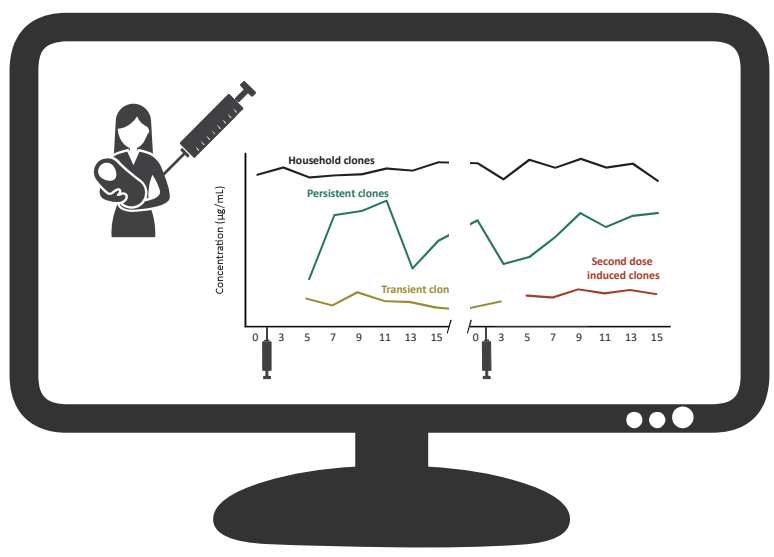
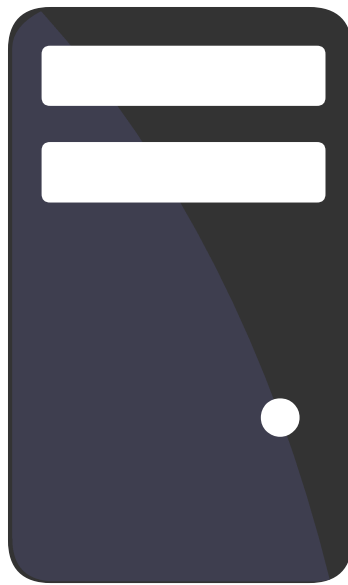
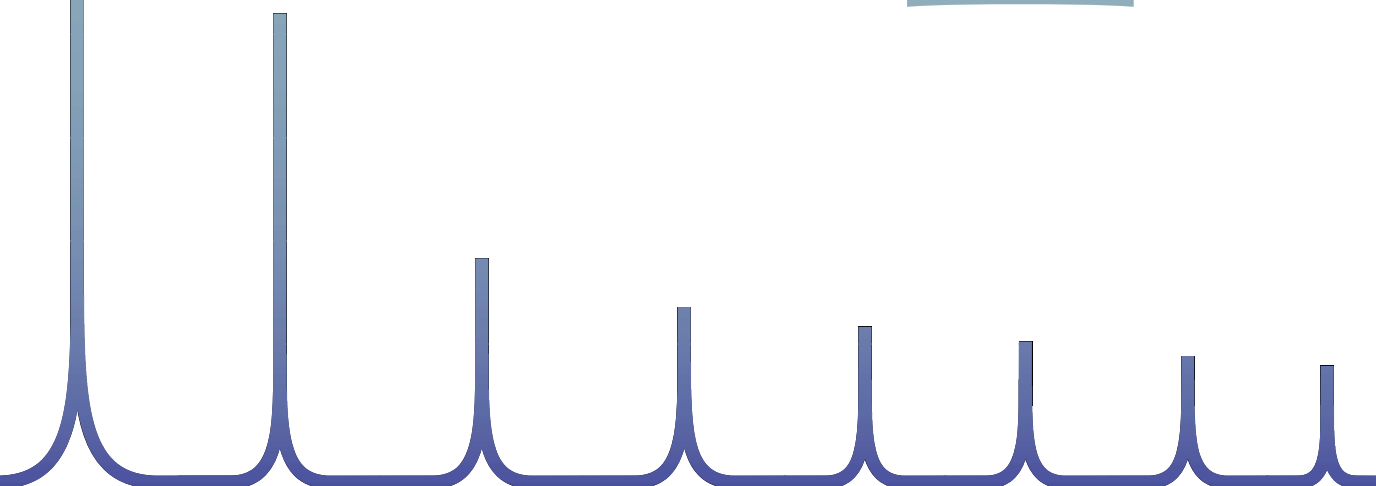


4



Exploring the human milk polyclonal IgA1 response to repeated SARS-CoV-2 vaccinations by LC-MS based Fab profiling

Sebastiaan C. de Graaf, Albert Bondt, Danique M.H. van Rijswijck, Hannah G. Juncker, Sien J. Mullenens, Mirjam J.A. Damen, Max Hoek, Britt J. van Keulen, Johannes B. van Goudoever, Albert J.R. Heck, Kelly A. Dingess

This chapter is based on work in the following manuscript (in preparation for submission):

PNAS (2021), 118:e2110996118, doi:10.1073/pnas.2110996118

Abstract

Upon vaccination against severe acute respiratory syndrome coronavirus 2 (SARS-CoV-2) humans will start to produce antibodies targeting virus specific antigens that will end up in circulation. In lactating women such antibodies will also end up in breastmilk, primarily in the form of secretory immunoglobulin A1 (SIgA1), the most abundant immunoglobulin (Ig) in human milk. Here we set out to investigate the SIgA1 clonal repertoire response to repeated SARS-CoV-2 vaccination, using a LC-MS fragment antigen-binding (Fab) clonal profiling approach. We analyzed the breastmilk of six donors from a larger cohort of 109 lactating mothers who received one of three commonly used SARS-CoV-2 vaccines. We quantitatively monitored the SIgA1 Fab clonal profile over 16 timepoints, from just prior to the first vaccination until 15 days after the second vaccination. In all donors, we detected a population of 89-191 vaccine induced clones. These populations were unique to each donor and heterogeneous with respect to individual clonal concentrations, total clonal titer, and population size. The vaccine induced clones were dominated by persistent clones (68%) which came up after the first vaccination and were retained or reoccurred after the second vaccination. However, we also observe transient SIgA1 clones (16%) which dissipated before the second vaccination, and vaccine induced clones which uniquely emerged only after the second vaccination (16%). These distinct populations were observed in all analyzed donors, regardless of the administered vaccine. Our findings suggest that while individual donors have highly unique human milk SIgA1 clonal profiles and a highly personalized SIgA1 response to SARS-CoV-2 vaccination, there are also commonalities in vaccine induced responses.

4.1 Introduction

IMMUNOGLOBULINS (Ig), or antibodies, are a key part of the adaptive immune response capable of specifically recognizing and binding to antigens derived from bacteria or viruses initiating and aiding in their neutralization. Every individual has a unique antibody repertoire generated by a magnitude of distinct antibody-producing B cells, with estimates ranging from 10^{13} to 10^{18} (1, 2). Throughout our lives these repertoires are built up by encountering a huge variety of pathogens and other foreign stimuli, which we are exposed to daily or at specific moments in time, such as vaccines. However, at a given moment in time there are likely only hundreds to thousands of different detectable antibodies in human serum and milk, and typically the top 50 most abundant Ig clones account for up to 90% of the complete Ig repertoire (3–5). In our first moments of life, we begin to build this repertoire and are provided passive immunity through breastfeeding, receiving in most cases our mother's own unique antibodies. After natural infection with severe acute respiratory syndrome coronavirus 2 (SARS-CoV-2), SARS-CoV-2 specific antibodies with neutralizing capacity are present in human milk and are thought to provide immunity to infants (6–12). The advantages of breastfeeding and the absence of vertical transmission of SARS-CoV-2 via human milk (6, 8, 13–15) have led to the advice of the WHO to encourage mothers to continue breastfeeding their infant during the COVID-19 pandemic (16). Recently, several SARS-CoV-2 vaccines have been widely administered to people around the world. While the accumulated evidence has shown that these vaccines are safe and effective also for pregnant and lactating women (17–22), this more vulnerable group was excluded from initial SARS-CoV-2 vaccine trials. Therefore, information regarding vaccine driven antibody development in lactating women is still rather limited. This information is beneficial for breastfeeding women to make a well-informed decision regarding vaccination to confer protection to not only themselves, but also their immune naïve infant (23). The most abundant Ig in human milk

is IgA at a concentration of 1.0-2.6 g/L being 10 to 100 times greater than IgG and IgM respectively (24, 25). IgA comes in two subclasses IgA1 and IgA2, with IgA1 typically being the more abundant subclass in human milk. We recently developed methods to study IgA1 clonal repertoires in human serum and milk. After affinity-purification, all IgA (IgA1 and IgA2) molecules from human serum or milk (4, 5) become bound to the affinity resins, whereafter we use specific enzymes to cleave IgA1 molecules selectively, yielding the fragment antigen binding (Fab) domains that harbor the complementarity determining regions. These Fabs are then subjected to intact mass analysis by LC-MS clonal profiling. This yields a clonal profile that typically contains several hundred unique clones, each identified by a specific LC-MS signature based on mass and retention time. We can quantify the human milk concentrations of each Fab clone by spiking in recombinant IgA1 mAb standards (4), enabling us to monitor the abundance of individual clones over time. Monitoring the human milk IgA1 clonal repertoire of healthy individuals, we observed that they are relatively simple, being dominated by just a few hundred to thousand different clones at a given time. These repertoires are unique and highly personalized as we do not observe the same clones in more than one donor. Furthermore, we found the human milk IgA1 repertoires of healthy donors to be very stable over time (4), whereas the clonal repertoires of individuals that experience serious illness, can undergo distinct and sudden changes (3, 26). Mothers that were previously infected with SARS-CoV-2 have significantly higher concentrations of spike specific IgA in their breastmilk than negative controls (9), and using LC-MS we were able to detect spike specific secretory IgA1 (SIgA1) Fab fragments in these donors. Interestingly, concentrations of spike specific IgA in human milk had little correlation with neutralization capability, and spike specific SIgA1 Fabs were of a relatively low concentration when compared to total SIgA1 in human milk. Other studies have also shown weak correlations between antibody titers and the frequency of recirculating memory B cells relative to a respective antigen (27). These findings suggest that high concentrations of antibodies may not

Chapter 4

4

be good predictors for effective viral recognition and binding. Detailed knowledge about the emergence and evolution of antibodies in response to vaccination could render better insights into the immunity they provide and thereby yield better predictors for its longevity and effectiveness. Here, we aim to expand the knowledge about the antibody response of lactating women following SARS-CoV-2 vaccination by investigating the IgA1 profiles of six individuals that received repeated mRNA-based or vector-based SARS-CoV-2 vaccines. Donors and their samples for this observational longitudinal case series were selected from a previously described cohort (28). Using LC-MS Fab clonal profiling, we monitored the abundance of individual IgA1 clones and studied the antibody response at a clonal level of detail. Novel in this study is that we use computational methods to detect IgA1 Fab clonal populations emerging after vaccination by eliminating all clones that were present before a response to vaccination could be expected. The human milk IgA1 clonal repertoires of six individual donors receiving one of three SARS-CoV-2 vaccines were longitudinally (at 16 timepoints), quantitatively monitored. All six donors had unique IgA1 clonal repertoires in which longitudinal changes were observed, with novel clonal populations emerging after both the initial and second vaccination. Our data reveals that antibody responses to vaccination are highly personalized traits and argues for monitoring antibody responses beyond the total Ig titer level, using a more detailed, personalized, and longitudinal approach.

4.2 Results

4.2.1 Vaccination results in a heterogeneous polyclonal response

In this observational longitudinal case series, we recorded the human milk IgA1 clonal profiles of six individual donors receiving either Comirnaty, Spikevax or Vaxzevria vaccines (**Figure 1**). We detected a total of 2553 clones across all donors, ranging

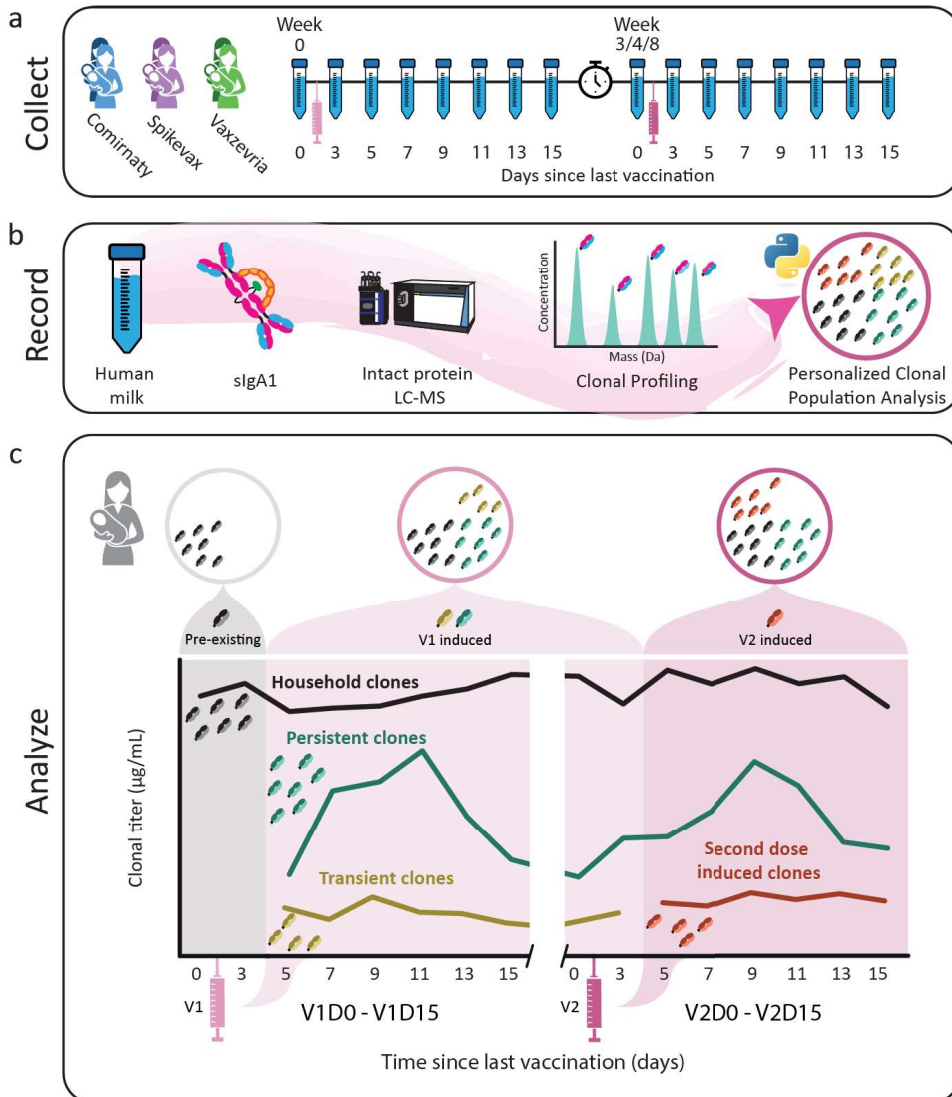


Figure 1: Figure Legend on next page.

between 229 and 505 unique clones per donor (Figure 2a), excluding clones that were only found at a single timepoint from all subsequent analysis to limit false discoveries. In line with our previous studies, there was virtually no overlap in the clonal repertoire between donors (only a single clone had an overlapping mass and retention time between donors). In contrast, overlap within each individual donor over the longitudinal sampling was exceptionally high (over 95% of clones were detected at

Chapter 4

Figure 1: Study Workflow. a) Human milk samples were obtained from six donors across 16 timepoints, from just prior to the first vaccination until 15 days after the second vaccination. Individual donors received one of three vaccines, BNT162b2/Comirnaty (blue), mRNA-1273/Spikevax (purple) or AZD1222/Vaxzevria (green). The sample collections are indicated by the tubes and each vaccination with a syringe. The clock indicates the gap in time between vaccinations. b) SlgA1 was affinity-purified from human milk. Subsequently, proteolytically formed SlgA1 Fab fragments were separated and analyzed by LC-MS to obtain a list of clones (i.e., Fab molecules with a unique mass/retention time pair). The concentration of each clone was retrieved at the sampled timepoints using two recombinant IgA internal standards. Clones were then assigned to populations based on their window of detection relative to vaccination, and these populations were analyzed for each donor individually. c) Illustrative examples of abundance profiles of clonal populations over time. The y-axis shows the clonal titer (i.e., the summed concentrations of the clones) for each population over time. Timepoints are referred to as for example V1D3, where D3 indicates the number of days since the last vaccination and V1 indicates the last vaccination. Clones were assigned to one of four populations based on their detection window relative to vaccination. The black line represents *household* clones, SlgA1 clones that were detected in one of the first two timepoints, before a response to vaccination could be expected based on analysis of the parent cohort. All other clonal population were absent from these time points and are considered vaccine induced clones. The remaining three populations designated are *persistent* (teal), *transient* (mustard) and *second dose induced* (maroon) clones. The transient population consists of clones that are only detected in the window V1D5 - V2D3. The persistent clones are clones that arise in the window V1D5 - V2D3 and are also detected after V2D3. Clones in the second dose induced population are clones that were not observed until after V2D3.

more than one timepoint).//

For all donors, the SlgA1 clonal repertoire was dominated by abundant clones that were already detected in the first (V1D0) or second (V1D3) milk sample, before a clonal response is expected as it is prior to or too close to vaccination, as also confirmed based on ELISA data (28) (**Figure S1**). These clones, which we term *household* clones (**Figure 1c, Figure S2**), accounted for 92% of the total SlgA1 *clonal titer* (the summed abundance of all clones) of all samples combined (**Figure 2b**) and 83-99% of the total SlgA1 clonal titer in any single sample. In each donor, we detected between 89 and 191 clones that emerged more than 3 days after the first vaccination (V1D5 and later) (**Figure 2a**). These clones, which we termed *vaccine induced clones* (**Figure 1c, Figure S2**), made up 31% of the total detected clones (793 out of 2553 clones, **Figure 2a**). These vaccine induced clones were comparatively low in abundance and made up a relatively small portion of the total SlgA1 clonal titer per sample (**Figure 2c**). Most of the vaccine induced clones emerged shortly after the first vaccination was administered: 47% of the vaccine induced clones (377 clones), were first observed between V1D5 and V1D7 (**Figure 2d**). This agreed with

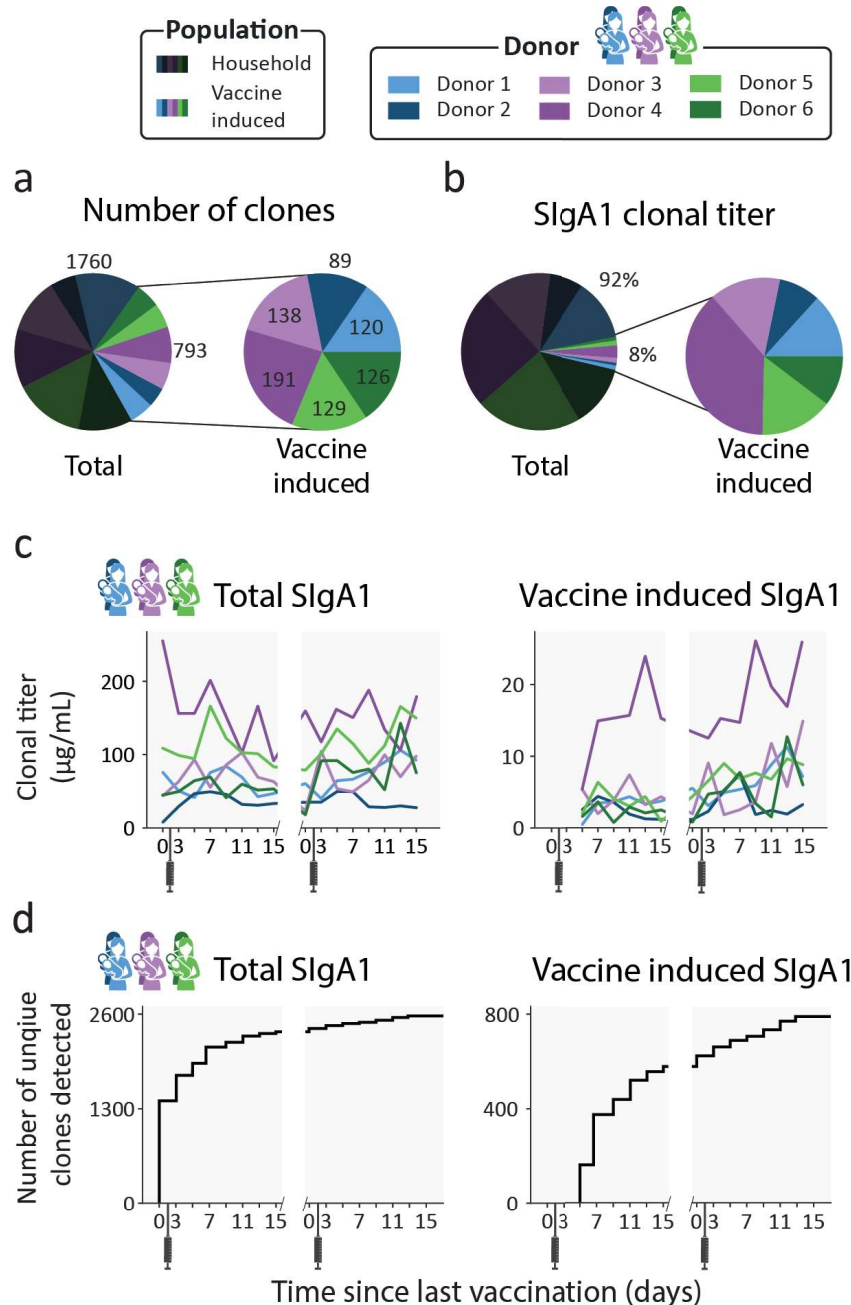


Figure 2: Emergence of novel clones after vaccination. a) Pie charts showing the number of unique clones designated as household (dark) and vaccine induced (light), colored per donor. Vaccine induced clones made up 31% of all detected clones (793 out of 2553 clones). b) Pie charts showing the percent total abundance the household clones (dark) and vaccine induced clones (light), colored per donor. c) Longitudinal changes in total IgA1 clonal titer (left) and vaccine induced IgA1 clonal titers (right) for each donor. Vaccine induced IgA1 clonal titers rise in response to the repeated vaccinations and make up an average of 7% of the total IgA1 clonal titer. d) Total number of unique clones detected over time (left) and number of unique vaccine induced clones (right). Novel clones emerge shortly after vaccination and by day 7 nearly half of all vaccine induced clones (377 out of 793) have been detected.

the ELISA findings for these same samples, where anti-spike IgA titers started rising around day 5, and further sharp increases were observed 9 days after vaccination (**Figure S1**).

4.2.2 Novel clonal populations emerge after the second vaccination in all donors

As the vaccines the donors received consist of two doses, we defined four clonal populations based on the window of detection relative to both vaccinations (**Figure 1c**, **Table S1**). The first population we termed above as *household* clones. These are IgA1 clones that were detected before a clonal response was expected, at V1D0 or V1D3. The previously described *vaccine induced* clones were categorized into three distinct populations: *transient*, *persistent*, and *second dose induced* clones. The transient and persistent populations are both made up of clones that were detected before timepoint V2D3 but were absent at the first two timepoints (V1D0 and V1D3). The transient clones were *only* detected in the time window from V1D5 to V2D3. Persistent clones arose in this same time window but were *also* detected after V2D3. Clones in the second dose induced population are clones that were first observed after V2D3. These four populations were observed in all donors. Persistent clones were the largest population: 21% of all detected clones were persistent clones (539 clones, **Figure 3a**), and persistent clones made up between 50 and 80% of donor specific vaccine induced clones (**Figure 3b**). The transient and second dose induced populations were much smaller and more diverse. The transient and second dose induced populations each make up 5% of all clones (126 and 128 clones respectively, **Figure 3a**), and 5-20% and 5-27% of donor specific vaccine induced clones (**Figure 3b**) respectively. When looking at the fractional clonal titer (i.e., the proportion a population contributed to the total IgA1 clonal titer at a single timepoint) over time, the behavior of these populations was remarkably similar between donors

(Figure 3c). The persistent clones dominated here too, as they made up the bulk of the vaccine induced clonal titer at nearly all timepoints and on average of 5.9% of the total IgA1 clonal titer. Transient and second dose induced populations accounted for a much smaller fraction (on average 0.7% and 1.7% respectively) of the total IgA1 clonal titer for any single sample (Figure 3c).

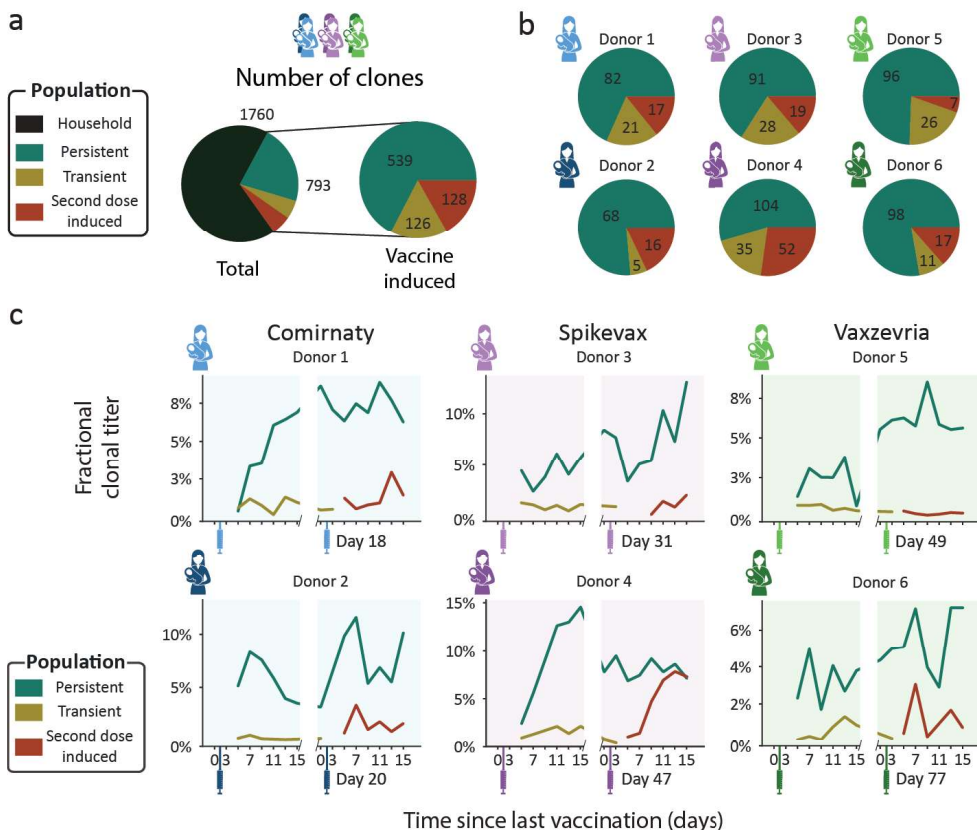


Figure 3: Clonal population analysis. a) Pie charts showing the total number of unique clones in each population. Clones were assigned to populations based on their detection window relative to the vaccination moments: persistent (teal), transient (mustard), and second dose induced clones (maroon). b) Pie charts showing the number of unique clones in each population per donor. Each pie chart shows data for a single donor (Comirnaty (2 blue donors), Spikevax (2 purple donors) and Vaxzevria (2 green donors)). c) Longitudinal changes in fractional clonal titer (i.e., fraction of the total clonal titer made up by each population) for the vaccine induced clonal populations. Vaccination moments are depicted as color-coded syringes. Each panel shows donor-specific, fractional clonal titers for the three vaccine induced populations. While all donors show a unique repertoire without overlapping clones, varying in number of clones and total clonal titer, when grouped into populations the responses are more consistent. Persistent clones make up the bulk of the vaccine induced IgA1 clonal titer at nearly every timepoint. The clonal titers of the transient and second dose induced populations account for a much smaller fraction of IgA1.

4.2.3 Clonal titer fluctuations can be driven by highly divergent clonal populations

From the ELISA analysis by Juncker et al. (28), donor 4 was identified as the strongest responder in terms of spike-specific IgA. This prompted us to have a closer look at this donor. Our analysis confirmed the strong response, as the vaccine induced clonal titer reached a peak concentration of 26.3 µg/mL, higher than any other donor (maximum 14.7 µg/mL, **Figure 2c**), and featured 191 unique clones, more than any other donor (maximum 138 clones, **Figure 2a**). Uniquely in donor 4, we observed that the second dose induced clonal titer increased comparably to the persistent clonal titer (**Figure 3c**), indicating that the clonal makeup of the response to the second vaccination was strongly divergent from the response to the initial vaccination. Despite looking very similar to the first phase of the biphasic response (**Figure 2c**), the second phase of the response was largely driven by the second dose induced population and not the persistent population that was induced by the first dose as the persistent population clonal titer remained relatively stable (**Figure 3c**). The second dose induced population that drives this second peak in the vaccine induced titer is the largest and most abundant in this study, consisting of 52 unique clones (**Figure 3**), peaking at over 10 µg/ml (**Figure S3**). Additionally, the second dose induced population made up 45-50% of the vaccine induced clonal titer and 39-44% of vaccine induced clones during the last 3 timepoints (**Figure 4**), demonstrating how seemingly similar titer fluctuations can be driven by highly divergent clonal populations. At these final timepoints, the persistent clonal titer had decreased to approximately half its peak value (**Figure S3**). However, we did not observe a similar decrease in the number of detected persistent clones suggesting either a simultaneous drop in the intensity of the individual persistent clones or a strong decrease in abundance of one or more dominant clones from this population. Inspection of the individual persistent clones revealed that at its peak (V1D13), the persistent population included three

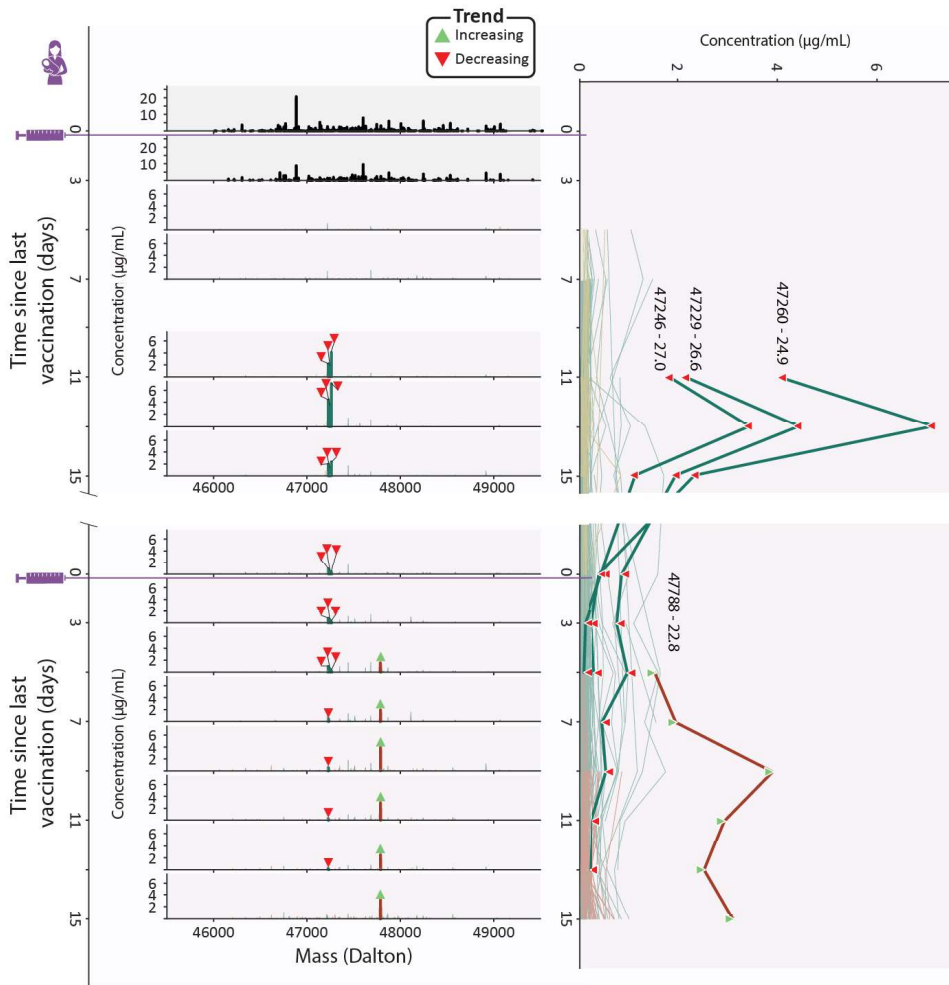


Figure 4: Clonal profile analysis for donor 4, a strong responder. Changes in the vaccine induced clonal profile for donor 4 are depicted, with the 4 most abundant vaccine induced clones annotated by their mass and retention time, highlighted in bold, with each timepoint annotated with a triangle indicating if the clone trends upwards or downwards in concentration over the course of this study. On the left we show mass profiles (S IgA1 clonal concentration in $\mu\text{g/mL}$) showing either household clones (top two profiles, in black) or vaccine induced clones (subsequent profiles, with individual clones colored according to their assigned population (persistent (teal), transient (mustard), and second dose induced clones (maroon)). Each peak indicates a single clone and each row a single timepoint. The line plot on the right shows the abundance of individual vaccine induced S IgA1 clones over all timepoints, colored by their population, with the same clones as the mass plots highlighted in bold, labeled with their mass and retention times and annotated with triangles indicating if the clone trends upwards or downwards in concentration throughout the study duration. The highlighted persistent clones are initially highly abundant, but their abundance decreases rapidly, and at the final timepoint none of them are detected. The highlighted second dose induced clone is part of a large and abundant population of second dose induced clones, which at the final timepoints make up 45-50% of the vaccine induced clonal titer.

Chapter 4

highly abundant clones which together made up 60% of the persistent clonal titer (**Figure 4**). While initially these highly abundant clones almost completely dictated the persistent clonal titer fluctuations, they quickly declined in abundance after an initial peak and eventually disappeared while the persistent clonal titer remained relatively stable (**Figure 4** and **Figure S2**), seemingly causing the persistent clonal titer drop between the first and second phase. A similarly dominant second dose induced clone was observed to increase in concentration as the three dominant persistent clones were decreasing at V2D5 (**Figure 4**). The abundance profile of this clone mirrored the upward trending second dose induced titer (**Figure S3**) and was the most abundant clone at the final timepoint, at 3.1 µg/mL (**Figure 4**). However, 37 other second dose induced clones are still detected at the last timepoint and as we saw with the persistent clones, it may be these lower abundant clones that persist in the long term. These dominant clones demonstrate how clonal titers fluctuations can be strongly influenced by a limited number of abundant clones. Sometimes these clones only amplify the behavior of their parent population, as with the highlighted second dose induced clone. However, they may paint a misleading picture by masking the cumulative behavior of the remaining, lower abundant, clones in the population. The clonal resolution of the LC-MS based Fab profiling method enables us to zoom in on individual clones and allows us to confirm the presence or absence of factors that drive polyclonal responses.

4

4.3 Discussion

The current body of knowledge about humoral immunity in response to infections and vaccinations are normally determined by ELISAs for total antigen-specific antibody titers and more recently by screening for antigen-specific B-cells. However, recent work by Wolf et al. (27) shows that the antibody titers are poor markers of the frequency of memory B cells after an infection. Therefore, alternative analyses

are needed to assess the basics of humoral immunity. We may gain new insights by uncovering when, how and why specific antibodies come up after an infection or vaccination. A first step in doing this is by monitoring individual clones and extracting patterns from clonal populations, as we demonstrate here. In this study, we detected a heterogeneous polyclonal response to vaccination, as distinct populations of novel clones emerged in every donor after vaccination. We defined three populations vaccine induced clones can be assigned to based on their window of detection relative to vaccination: transient, persistent and second dose induced clones (**Figure 1c, Figure S2**). These populations were not only observed in all donors, but also behaved remarkably similar relative to each other, as the persistent population was dominant both in terms of clonal titer and size, regardless of which vaccine the donor had received. As the donors in this study had not been exposed to SARS-CoV-2 prior to vaccination, the clonal response to the first vaccination can be considered the primary response: a first generation of antibodies, having undergone little to no somatic hypermutation (29). The dominant persistent clones we observe might be the effective portion of the primary response, which are encoded in long lived plasmablasts or memory B cells that proliferate quickly in response to restimulation with the same antigen whereas the transient population could be the ineffective portion of the primary response. The response to the second vaccination can then be considered the secondary response. In every donor, we observed a population of novel clones emerge during this secondary response. In at least one donor, donor 4, the secondary response had a strongly divergent clonal makeup from the primary response, as it was not predominantly driven by clones induced upon the first vaccine dose but largely by a completely novel clonal population. These novel clones may be the result of a completely new gene recombination but could also be the result of somatic hypermutation of transient or persistent clones, as even small mutations are likely to cause shifts in mass and retention time. Alternatively, they could be clones that escaped detection during the primary response or clones that were derived from

Chapter 4

previously undetected clones through somatic hypermutation or isotype switching, as our profiling method in this study was limited to IgA1. While more extensive sequence information is needed to definitively determine the genetic and cellular origin of circulating clones, the second dose induced clones in this study seemingly did not emerge faster than the transient clones, possibly indicating they are not maturations of the first batch of B cells. However, given the small sample size in this study, we are unable to sufficiently answer these questions. In the parent study of this cohort, spike specific IgAs were longitudinally monitored by ELISA. A biphasic antibody response to SARS-CoV-2 vaccination was observed for spike-specific IgA in these samples, with an accelerated response after the second vaccination, in line with expectations based on leading theories on humoral immune responses (29). We were able to confirm a number of these findings from our case series analysis of this cohort. From both the ELISA and Fab profiling data, donor 4 could be identified as a strong responder, with an observed biphasic response irrespective of analysis type. These confirmations, however, could only be made qualitatively. Quantitatively, we observed a discrepancy between the reported ELISA and measured clonal titers. We believe there are several factors contributing to these discrepancies. First, the applied ELISA measured IgA1 and IgA2, whereas our profiling method detect only IgA1 (9, 28). Furthermore, the ELISA measured spike-specific IgA titers, using a pre-fusion stabilized variant of the spike protein sequence termed 2P (30). Thus, clones that do not bind to the 2P spike protein variant, but perhaps to other components of the vaccine, will not be detected. Similarly, weak binders may be underrepresented in affinity-based assays. As a recent study showed that low rather than high affinity antibodies delivered greater antibody-mediated receptor activity through increased receptor clustering (31), these low affinity clones may be of particular importance. To date, it is often thought that highly efficient neutralizing antibodies would perhaps not be among the most abundant clones. However, at the current stage of implementation the most reliable detection and quantitation through LC-MS is limited to relatively

abundant clones, and low abundant clones likely exist at concentrations below our limit of detection. One way to study these low abundant clones is through fractionation or purification. While there is value in retaining biological context by minimizing purification, simultaneous analysis of the sample in an enriched form can enable a more targeted look at clones of interest or provide us with contextual information about clones in our sample such as binding affinity. For example, in a recent study van Rijswijck et al. (26) analyzed serum samples of SARS-CoV-2 patients, with and without affinity purification, and combined the results to yield information about the cross-reactivity of individual clones to different SARS-CoV-2 variants of concern. This illustrates how the ability to identify and track clones between samples and experiments can be used to obtain functional information about individual clones, and how we can relate this information back to the original abundance profile. Future applications of LC-MS fab profiling hold the promise of high throughput characterization of antibody repertoires, allowing for a greater understanding of the mechanisms related to antibody mediated immunity and defining immune signatures that predict how an individual will respond to future encounters with similar antigens. We imagine this to have future applications similar to HLA phenotypes for organ transplants or genetic markers for cancer treatment. In addition to defining such “biomarkers” for individual patients, we could identify markers of efficacy for individual clones, potentially enabling the direct identification of potential therapeutic antibodies from polyclonal samples. We believe studies like this pave the way to elucidate the mechanisms involved in mounting an effective antibody response and can lead to future targeted efforts to find potential therapeutic candidates.

Chapter 4

4.4 Methods

4.4.1 Study design

In this study we used samples from an existing prospective longitudinal study COVID MILK – POWER MILK (28). All participants were subjected to longitudinal analysis of specific antibodies against the SARS-CoV-2 spike-protein by ELISA and general IgA1 Fab clonal profiling in human milk after vaccination against COVID-19 with BNT162b2/Comirnaty developed by Pfizer-BioNTech, mRNA-1273/Spikevax developed by Moderna or AZD1222/Vaxzevria developed by Oxford/AstraZeneca. Ethical approval was acquired from an Independent Ethics Committee (2020.425/NL74752.029.20).

The study was conducted in accordance with the principles of the declaration of Helsinki and the ICH GCP Guidelines, and the Regulation on Medical Research involving Human subjects.

4

4.4.2 Subjects

Details concerning subjects have been extensively described (28). Briefly, lactating women in the Netherlands receiving one of the above-described SARS-CoV-2 vaccines were eligible to participate and were recruited through social media platforms. There were no exclusion criteria. All participants were requested to send their vaccination certificate, including the type of vaccination and lot number. From the larger study a subset of 2 women per vaccine group were selected based on the following criteria: 1) a pre-vaccine milk sample was available, 2) data from an enzyme-linked immunosorbent assay (ELISA) with the SARS-CoV-2 spike protein for human milk IgA was available and indicated high spike-specific IgA titers. Written informed consent was obtained from all participants.

4.4.3 Sample collection

Sample collection was performed between January 2021 and July 2021. Human milk samples were collected longitudinally over a period of up to 95 days (**Figure 1**). In this study, 16 samples of human milk were analyzed per lactating woman. These samples were collected according to the following schedule: one sample before the first vaccination and one sample on days 3, 5, 7, 9, 11, 13, and 15 after the first vaccination. This schedule was the same for the second vaccination (**Table S1**). Participants were instructed to empty one breast in the morning, before the first feeding moment, and collect 5 mL of milk after mixing the milk. Participants were requested to store the milk samples in the home freezer. Samples were transported back to the lab on dry ice and remained at -80 until analysis (9, 28).

4.4.4 Fab clonal profiling from human serum and milk

IgA enrichment, capture, and digestion

Methods for IgA1 Fab profiling have previously been extensively detailed (3, 4). Briefly, all IgA was captured using CaptureSelect IgA affinity matrix (Thermo Fisher Scientific). Human milk samples were assumed to contain 0.8 µg/µL SIgA and added to excess amount of bead slurry, PBS, and 200 ng of the monoclonals anti-CD20 mIgA1 (7D8-IgA1) and anti-cMET (5D5v2-IgA1). These monoclonals were used as internal standards for quantification, and were a gift from Genmab (Utrecht, NL). Samples were incubated followed by removal of the flow through, containing all non-IgA human milk components. The samples were then washed several times and IgA was digested overnight with the O-glycopeptidase from Akkermansia muciniphila, OgpA (OpeRATOR®, Genovis, Llund, Sweden). Digestion was performed using 40 U SialEXO (a sialidase cocktail to remove sialic acids from the O-glycans) and 40 U of OgpA enzyme, and incubated overnight at 37 °C, in an Eppendorf thermal shaker (Eppendorf, The Netherlands). Following overnight digestion with OgpA, Ni-

Chapter 4

NTA agarose slurry was added to the samples to bind the enzyme and incubated for 30 min. Finally, the flowthrough, containing the IgA1 Fabs, was collected by centrifugation.

Fab profiling by LC-MS

The LC-MS and data processing approaches as described by Bondt et al. were applied (3, 4). In short, the collected Fab samples were separated by reversed phase liquid chromatography on a Thermo Scientific Vanquish Flex UHPLC instrument, equipped with a 1 mm x 150 mm MAbPac analytical column, directly coupled to an Orbitrap Fusion Lumos Tribrid mass spectrometer (Thermo Fisher Scientific, San Jose, California, USA). The column preheater and the analytical column chamber were heated to 80°C during chromatographic separation. Fab samples were injected as 10 µL and subsequently separated over a 62 min gradient at a flow rate of 150 µL/min. The gradient elution was achieved using mobile phases A (0.1% HCOOH in Milli-Q HOH) and B (0.1% HCOOH in CH3CN), see previous publications for details (3, 4). The instrument was operating in Intact Protein and “Low Pressure” mode for the acquisition of MS data, with a spray voltage of 3.5 kV set from minute 2 to minute 50 of the gradient. The ion transfer tube temperature was set at 350°C, vaporizer temperature at 100°C, sheath gas flow at 15, auxiliary gas flow at 5, and source-induced dissociation (SID) was set at 15 V. Spectra were recorded with a resolution setting of 7,500 (@ 200 m/z) in MS1. Scans were acquired in the range of 500–4,000 m/z with an AGC target of 250% and a maximum injection time set to 50 ms. For each scan 5 µscans were recorded.

4

IgA1 clonal profiling data analysis

Intact masses were retrieved from the generated RAW files using BioPharmaFinder 3.2 (Thermo Scientific). Deconvolution was performed using the ReSpect algorithm

between 5 and 57 min using 0.1 or 0.3 min sliding windows with a 25% offset, a merge tolerance of 30 ppm, and noise rejection set to 95%. The output mass range was set from 10,000 to 100,000 with a target mass of 48,000 and mass tolerance 30 ppm. Charge states between 10 and 60 were included and the Intact Protein peak model was selected. Further data analysis was performed using Python 3.9.13 (with libraries: Pandas 1.4.4 (32), NumPy 1.21.5 (33), SciPy 1.9.1 (34), Matplotlib 3.5.2 (35) and Seaborn 0.11.2). Masses of the BioPharmaFinder identifications (components) were recalculated using an intensity weighted mean considering only the most intense peaks comprising 90% of the total intensity. Using the mAb standards, the intensity was normalized, a relative mass shift was applied to minimize the mass error and a retention time shift was applied to minimize deviation between runs. Components between 45 and 53 kDa with the most intense charge state above m/z 1000 and a score of at least 40 were considered Fab portions of IgA1 clones. The clones in samples of the same donor were matched between runs using average linkage (unweighted pair group method with arithmetic mean UPGMA) L^∞ distance hierarchical clustering. Flat clusters were formed based on a cophenetic distance constraint derived from a mass and retention time tolerance which were 2 Da and 1 min respectively. Clones within a flat cluster were considered identical between runs. Clones that were only detected at a single timepoint within a donor were excluded from the analysis. Clones were assigned to populations according to their detection window relative to vaccination as outlined in **Figure S2**.

4.5 Acknowledgements

We would like to sincerely thank all the mothers who participated and all students and research assistants who helped with this study.

Chapter 4

4.5.1 Data Availability

The mass spectrometry proteomics data have been deposited to the MassIVE repository with the dataset identifier XXXX.

4.5.2 Trial registration

This research project was registered at the Dutch Trial Register on May 1st, 2020, number: NL 8575, URL: <https://onderzoekmetmensen.nl/nl/trial/23001>.

4.5.3 Funding statement

This research received funding through the Netherlands Organization for Scientific Research (NWO) TTW project 15575 (SCdG and AJRH), the ENPPS.LIFT.019.001 project (AJRH) and the Roadmap Program X-omics 184.034.019 (AJRH). This research received further support by Stichting Steun Emma Kinderziekenhuis. MJvG acknowledges the Amsterdam Infection and Immunity Institute for funding this work through the COVID-19 grant (24175). KAD acknowledges the Amsterdam Reproduction and Development Institute for funding this work though the AR&D grant (V.000296).

4

4.5.4 Declaration of Interests

JBvG is the founder and director of the Dutch National Human Milk Bank and a member of the National Health Council. JBvG has been a member of the National Breastfeeding Council from March 2010 to March 2020.

4.6 Author Contributions

KAD, JBvG and AJRH conceived the ideas and jointly designed the study and experiments. KAD, MH, DMHvR, MJAD and AB performed all experiments. SCdG per-

formed the data analysis. HGJ, SJM, BJvK and JBvG collected all samples. SCdG, KAD, AB and AJRH wrote the manuscript, all others provided edits. AJRH and JBvG provided resources and funding for the project. All authors contributed to the article and approved the submitted version.

4.A Supplementary material

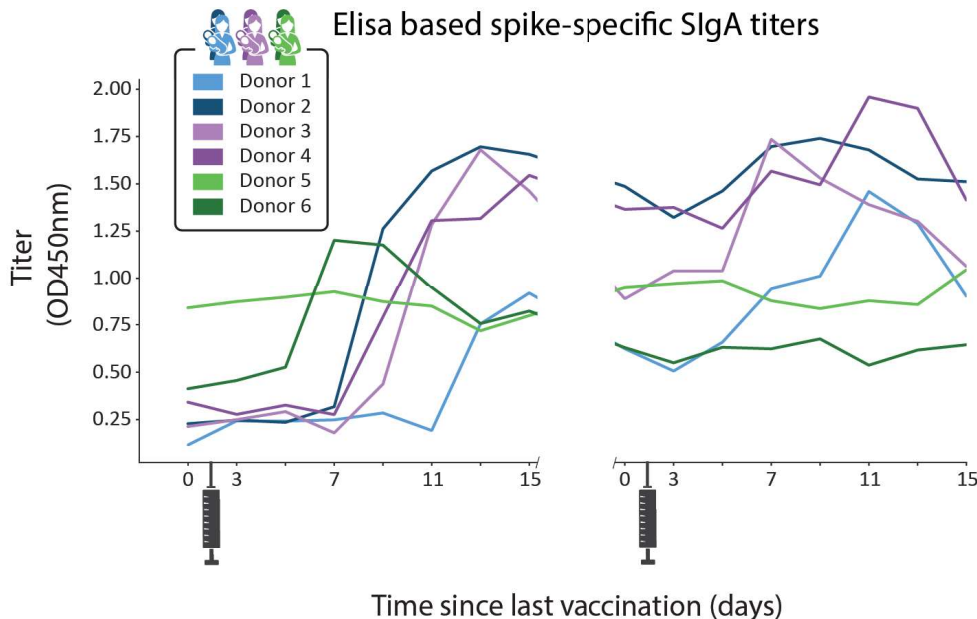
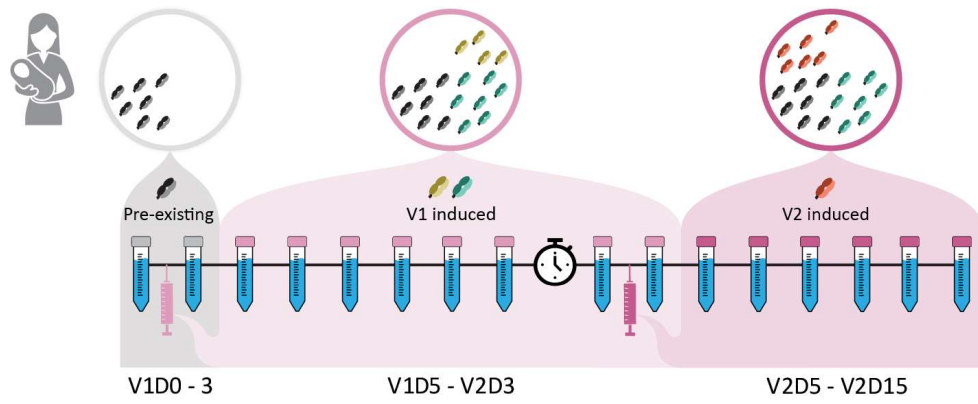


Figure S1: Quantified ELISA Spike-specific IgA titers. A biphasic antibody response to SARS-CoV-2 vaccination was observed for spike-specific IgA, with an accelerated response after the second vaccination. Original data from Juncker et al. (28).



4

		First detection		Last detection	
		min	max	min	max
Household		V1D0	V1D3	V1D0	V2D15
Vaccine induced	Transient	V1D5	V2D3	V1D5	V2D3
	Persistent	V1D5	V2D3	V2D5	V2D15
	Second dose induced	V2D5	V2D15	V2D5	V2D15

Figure S2: Clonal population inclusion criteria. Description of the criteria used to assign clones to the designated clonal populations based on their first and last detection moment (i.e., their detection window) relative to vaccination. Time windows are colored by appearance of clones relative to vaccination. Grey window (V1D0 – V1D3): Not attributed to vaccination. Light pink window (V1D5 – V2D3): Attributed to the first vaccination. Dark pink window (V2D5 – V2D15): Attributed to the second vaccination. Clones not detected in the first window were considered vaccine induced clones, and further assigned as follows: Clones first detected in the light pink window were considered transient clones if they were only detected in the light pink window, or persistent clones if they were detected in the dark pink window as well. Clones first detected in the dark pink window were considered second dose induced clones.

Chapter 4

4

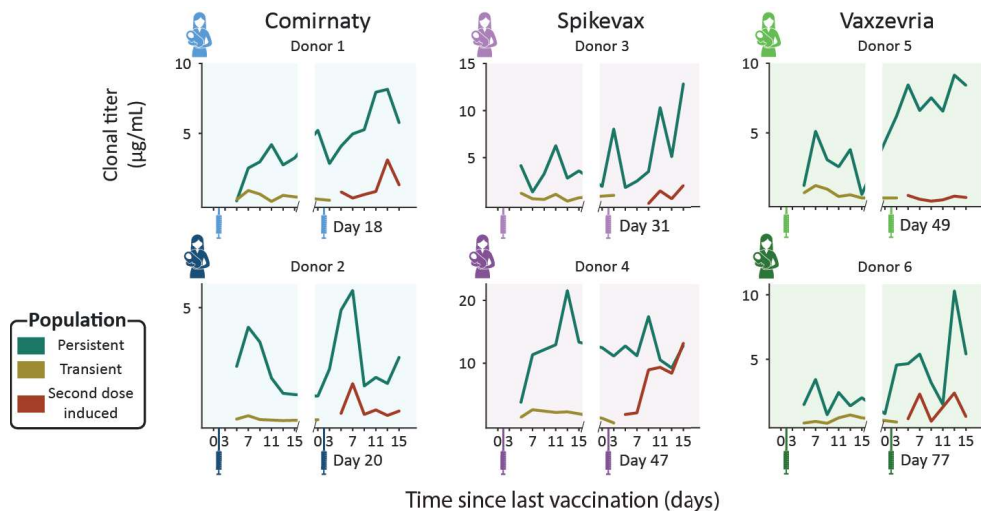


Figure S3: Longitudinal changes in absolute clonal titers for the vaccine induced populations. Each panel shows the population clonal titer (i.e., the summed concentrations of the individual IgA1 clones) for our three assigned, vaccine induced populations: Persistent clones (teal), transient (mustard) and second dose induced (maroon). Each panel shows data for a single donor (Comirnaty (2 blue donors), Spikevax (2 purple donors) and Vaxzevria (2 green donors)). Vaccination moments are depicted as color-coded syringes. Each panel shows donor-specific, clonal titers for the three vaccine induced populations. While all donors show a unique repertoire without overlapping clones, varying in number of clones and total clonal titer, when grouped into populations the responses are more consistent. Persistent clones make up the bulk of the vaccine induced IgA1 clonal titer at nearly every timepoint. The clonal titers of the transient and second dose induced populations account for a much smaller fraction of IgA1.

Donor number	Day	Label	Comirnaty		Spikevax		Vaxzevria	
			1	2	3	4	5	6
0	V1D0	0	0	0	0	0	0	0
First vaccination moment								
3	V1D3	3	3	3	3	3	3	3
5	V1D5	5	5	5	5	5	5	5
7	V1D7	7	7	7	7	7	7	7
9	V1D9	9	9	9	9	9	9	9
11	V1D11	11	11	11	11	11	11	11
13	V1D13	13	13	13	13	13	13	13
15	V1D15	<u>17</u>	15	NA	<u>17</u>	<u>17</u>	15	
<i>Suggested time between vaccinations</i>			21		28		54	
0	V2D0	18	20	31	NA	49	77	
Second vaccination moment								
3	V2D3	<u>22</u>	<u>24</u>	34	50	52	80	
5	V2D5	24	26	36	52	54	82	
7	V2D7	26	28	38	54	56	84	
9	V2D9	28	30	40	56	58	86	
11	V2D11	30	32	42	58	60	88	
13	V2D13	32	34	44	60	62	90	
15	V2D15	34	36	<u>48</u>	<u>63</u>	<u>66</u>	<u>95</u>	

Table S1: Sampling schedule for each donor. The “Day” column indicates the number of days between the last vaccination and the collection of each sample. The “Label” column indicates the label that is to refer to each sample in this manuscript. These are constructed as follows: for a sample labeled V1D3, D3 indicates the number of days since the last vaccination and V1 indicates the last vaccination received by the donor, so this sample was taken three days after the first vaccination. Samples collected just before vaccination are referred to as day 0 (i.e., V1D0 and V2D0). The actual days samples were collected from each individual donor are indicated as the number of days between the first vaccination and each sample collection. For some samples, the number of days between sample collection and the preceding sample collection deviated slightly from the schedule, these samples were underlined. NA indicates that the sample was collected but a date was not recorded. Blank spaces indicate that no sample was collected. The parent study included a follow-up sample, V2D70, for donor 2, 3 and 4. For donor 4, sample V2D15 was lost, and the follow-up sample was used instead. To unify the number of samples analyzed per donor per population, we excluded the remaining 2 follow-up samples from our analysis. The original study refers to donor 1-6 as PM2272, PM2183, PM2387, PM0281, PM0287 and PM0267 respectively.

Chapter 4

References

- [1] Bryan Briney, Anne Inderbitzin, Collin Joyce, and Dennis R. Burton. Commonality despite exceptional diversity in the baseline human antibody repertoire. *Nature*, 566(7744):393–397, 2019. ISSN 1476-4687. doi: 10.1038/s41586-019-0879-y.
- [2] Harry W. Schroeder. Similarity and divergence in the development and expression of the mouse and human antibody repertoires. *Developmental and Comparative Immunology*, 30(12):1119–135, 2006. ISSN 0145305. doi: 10.1016/j.dci.2005.06.006.
- [3] Albert Bondt, Max Hoek, Sem Tamara, et al. Human plasma IgG1 repertoires are simple, unique, and dynamic. *Cell Systems*, 12(12):1131–11435, 2021. ISSN 24054720. doi: 10.1016/j.cels.2021.08.008.
- [4] Albert Bondt, Kelly A. Dingess, Max Hoek, Danique M. H. van Rijswijk, and Albert J. R. Heck. A direct ms-based approach to profile human milk secretory immunoglobulin A (IgA1) reveals donor-specific clonal repertoires with high longitudinal stability. *Frontiers in Immunology*, 12:5190, 2021. ISSN 1664-3224. doi: 10.3389/fimmu.2021.789748.
- [5] Kelly A. Dingess, Max Hoek, Danique M.H. van Rijswijk, et al. Identification of common and distinct origins of human serum and breastmilk IgA1 by mass spectrometry-based clonal profiling. *Cellular and molecular immunology*, 20(1), 2023. ISSN 2042-0226. doi: 10.1038/s41423-022-00954-2.
- [6] Yunzhu Dong, Xiangyang Chi, Huang Hai, et al. Antibodies in the breast milk of a maternal woman with covid-19. *Emerging microbes and infections*, 9(1):1467–1469, 2020. ISSN 2222-1751. doi: 10.1080/22221751.2020.1780952.
- [7] Alisa Fox, Jessica Marino, Fatima Amanat, et al. Robust and specific secretory IgA against SARS-CoV-2 detected in human milk. *iScience*, 23(11), 2020. ISSN 2589-0042. doi: 10.1016/j.isci.2020.101735.
- [8] Ryan M. Pace, Janet E. Williams, Kirsi M. Järvinen, et al. Characterization of SARS-CoV-2 RNA, antibodies, and neutralizing capacity in milk produced by women with covid-19. *mBio*, 12(1):1–11, 2021. ISSN 2150-7511. doi: 10.1128/mbio.03192-20.
- [9] Britt J. van Keulen, Michelle Romijn, Albert Bondt, et al. Human milk from previously COVID-19-infected mothers: The effect of pasteurization on specific antibodies and neutralization capacity. *Nutrients*, 13(5), 2021. ISSN 2072-6643. doi: 10.3390/nu13051645.
- [10] Lars Bode, Kerri Bertrand, Julia A. Najera, et al. Characterization of SARS-CoV-2 antibodies in human milk from 21 women with confirmed COVID-19 infection. *Pediatric research*, 2022. ISSN 1530-0447. doi: 10.1038/s41390-022-02360-w.
- [11] Cibele Wolf Lebrão, Manuela Navarro Cruz, da Mariliza Henrique Silva, et al. Early identification of IgA anti-SARS-CoV-2 in milk of mother with COVID-19 infection. *Journal of human lactation: official journal of International Lactation Consultant Association*, 36(4):609–613, 2020. ISSN 1552-5732. doi: 10.1177/0890334420960433.
- [12] Hannah G. Juncker, M. Romijn, Veerle N. Loth, et al. Human milk antibodies against SARS-CoV-2: A longitudinal follow-up study. *Journal of human lactation: official journal of International Lactation Consultant Association*, 37(3):485–491, 2021. ISSN 1552-5732. doi: 10.1177/08903344211030171.
- [13] Jogender Kumar, Jitendra Meena, Arushi Yadav, and Praveen Kumar. SARS-CoV-2 detection in human milk: A systematic review. *The journal of maternal-fetal and neonatal medicine: the official journal of the European Association of Perinatal Medicine, the Federation of Asia and Oceania Perinatal Societies, the International Society of Perinatal Obstetricians*, 35(25), 2022. ISSN 1476-4954. doi: 10.1080/14767058.2021.1882984.
- [14] Paul Krogstad, Deisy Contreras, Hwee Ng, et al. No evidence of infectious SARS-CoV-2 in human milk: Analysis of a cohort of 110 lactating women. *medRxiv: the preprint server for health sciences*, 2021. doi: 10.1101/2021.04.05.21254897.
- [15] Christina Chambers, Paul Krogstad, Kerri Bertrand, et al. Evaluation for SARS-CoV-2 in breast milk from 18 infected women. *JAMA*, 324(13):1347–1348, 2020. ISSN 1538-3598. doi: 10.1001/jama.2020.15580.
- [16] World Health Organization. Breastfeeding and COVID-19: scientific brief, 23 June 2020. Technical report, 2020.

- [17] Hannah G. Juncker, Sien J. Mullenens, Marit J. van Gils, et al. Comparison of sars-cov-2-specific antibodies in human milk after mrna-based covid-19 vaccination and infection. *Vaccines*, 9(12), 2021. ISSN 2076-393. doi: 10.3390/vaccines9121475.
- [18] S.J.M. Zilver, C.J.M. de Groot, M. Grobbee, et al. Vaccination from the early second trimester onwards gives a robust sars-cov-2 antibody response throughout pregnancy and provides antibodies for the neonate. *International journal of infectious diseases : IJID : official publication of the International Society for Infectious Diseases*, 130, 2023. ISSN 1878-3511. doi: 10.1016/j.ijid.2023.02.022.
- [19] Winnie Fu, Brintha Sivajohan, Elisabeth McClymont, et al. Systematic review of the safety, immunogenicity, and effectiveness of covid-19 vaccines in pregnant and lactating individuals and their infants. *International journal of gynaecology and obstetrics: the official organ of the International Federation of Gynaecology and Obstetrics*, 156(3):406–417, 2022. ISSN 1879-3479. doi: 10.1002/ijgo.14008.
- [20] Denise J. Jamieson and Sonja A. Rasmussen. An update on covid-19 and pregnancy. *American journal of obstetrics and gynecology*, 226(2):177–186, 2022. ISSN 1097-6868. doi: 10.1016/j.ajog.2021.08.054.
- [21] Tom T. Shimabukuro, Shin Y. Kim, Tanya R. Myers, et al. Preliminary findings of mrna covid-19 vaccine safety in pregnant persons. *The New England journal of medicine*, 384(24):2273–2282, 2021. ISSN 1533-4406. doi: 10.1056/nejmoa2104983.
- [22] Raffaele Falsaperla, Guido Leone, Maria Familiari, and Martino Ruggieri. Covid-19 vaccination in pregnant and lactating women: a systematic review. *Expert review of vaccines*, 20(12):1619–1628, 2021. ISSN 1744-8395. doi: 10.1080/14760584.2021.1986390.
- [23] A. Katharina Simon, Georg A. Hollander, and Andrew McMichael. Evolution of the immune system in humans from infancy to old age. *Proceedings of the Royal Society B: Biological Sciences*, 282(1821), 2015. ISSN 14712954. doi: 10.1098/rspb.2014.3085.
- [24] Matylda Czosnykowska-ukacka, Jolanta Lis-Kuberka, Barbara Królik-Olejnik, and Magdalena Orczyk-Pawiowicz. Changes in human milk immunoglobulin profile during prolonged lactation. *Frontiers in Pediatrics*, 8:428, 2020. ISSN 22962360. doi: 10.3389/fped.2020.00428.
- [25] Bo Lönnerdal, Peter Erdmann, Sagar K. Thakkar, Julien Sauser, and Frédéric Destaillats. Longitudinal evolution of true protein, amino acids and bioactive proteins in breast milk: a developmental perspective. *The Journal of nutritional biochemistry*, 41:1–11, 2017. ISSN 1873-4847. doi: 10.1016/j.jnutbio.2016.06.001.
- [26] Danique M.H. van Rijswijk, Albert Bondt, Max Hoek, et al. Discriminating cross-reactivity in polyclonal igg1 responses against sars-cov-2 variants of concern. *Nature Communications* 2022 13:1, 13(1):1–10, 2022. ISSN 2041-1723. doi: 10.1038/s41467-022-33899-1.
- [27] Carla Wolf, Sebastian Köppert, Noémi Becza, et al. Antibody levels poorly reflect on the frequency of memory b cells generated following sars-cov-2, seasonal influenza, or ebv infection. *Cells*, 11(22), 2022. ISSN 2073-4409. doi: 10.3390/cells11223662.
- [28] Hannah G. Juncker, Sien J. Mullenens, Eliza J.M. Ruhé, et al. Comparing the human milk antibody response after vaccination with four covid-19 vaccines: A prospective, longitudinal cohort study in the netherlands. *EClinicalMedicine*, 47, 2022. ISSN 2589-5370. doi: 10.1016/j.eclinm.2022.101393.
- [29] Jr Charles A Janeway, Paul Travers, Mark Walport, and Mark J Shlomchik. Immunological memory. In *Immunobiology: The Immune System in Health and Disease*. New York, 5 edition, 2001.
- [30] Soo Seok Hwang, Jaechul Lim, Zhibin Yu, et al. Cryo-em structure of the 2019-ncov spike in the prefusion conformation. *Science (New York, N.Y.)*, 367(6483):1255–1260, 2020. ISSN 1095-9203. doi: 10.1126/science.abb2507.
- [31] Xiaojie Yu, Christian M. Orr, H. T. Claude Chan, et al. Reducing affinity as a strategy to boost immunomodulatory antibody agonism. *Nature*, 2023. ISSN 1476-4687. doi: 10.1038/s41586-022-05673-2.
- [32] Wes McKinney. Data structures for statistical computing in python. *Proceedings of the 9th Python in Science Conference*, pages 56–61, 2010. doi: 10.25080/majora-92bf1922-00a.
- [33] Stéfan Van Der Walt, S. Chris Colbert, and Gaël Varoquaux. The numpy array: A structure for efficient numerical computation. *Computing in Science and Engineering*, 13(2):22–30, 2011. ISSN 15219615. doi: 10.1109/mcse.2011.37.

Chapter 4

- [34] Pauli Virtanen, Ralf Gommers, Travis E. Oliphant, et al. Scipy 1.0: fundamental algorithms for scientific computing in python. *Nature Methods*, 17(3):261–272, 2020. ISSN 15487105. doi: 10.1038/s41592-019-0686-2.
- [35] John D. Hunter. Matplotlib: A 2d graphics environment. *Computing in Science and Engineering*, 9(3):90–95, 2007. ISSN 15219615. doi: 10.1109/mcse.2007.55.